Chapter 3

Materials and Methods

3 Work methodology

The following flowchart provides a schematic of the work methodology with chapter-wise details.

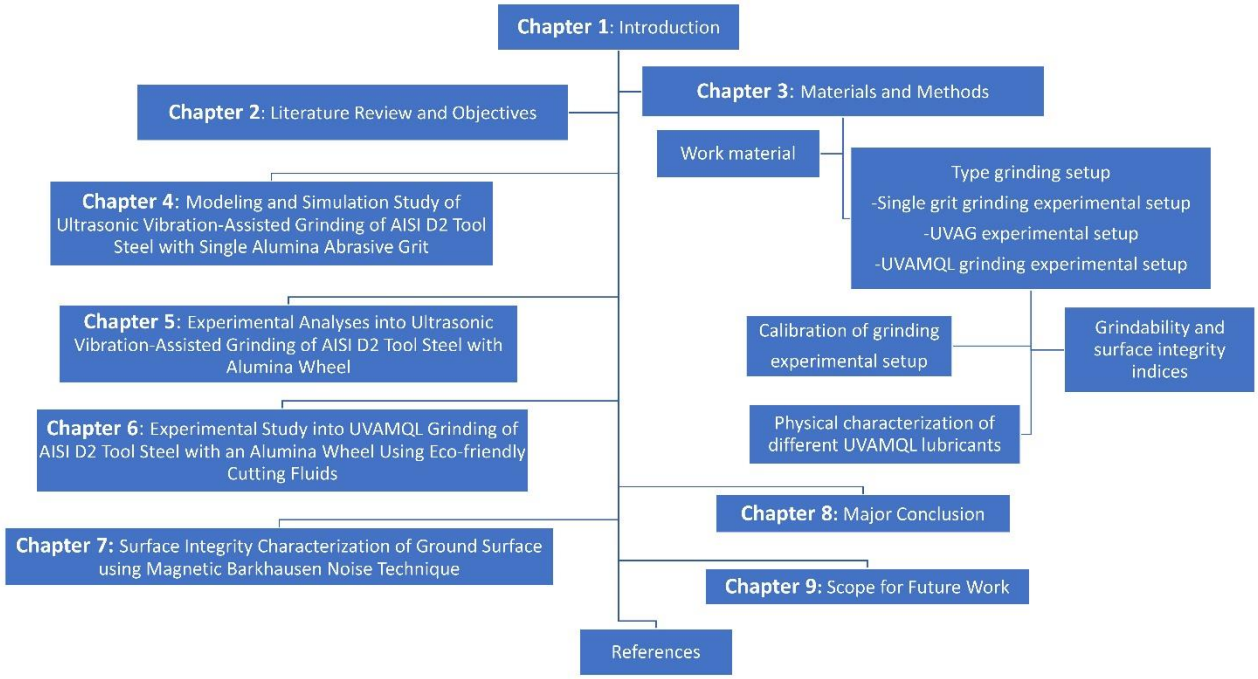

Figure 3.1 Work-methodology flow chart

3.1 Work material selection

The workpiece material employed for this research work is AISI D2 tool steel with dimensions of $70^{L}\times10^{T}\times15^{W}$ mm. AISI D2 tool steel is a crucial material for high-precision industrial applications such as moulds, punches, and dies; commercial cutting tools; gauges; machinery components prone to wear; injection screws; aerospace; automobile sectors; healthcare instruments; construction and fabrication equipment [246]. This is owing to its outstanding characteristics, which include greater temperature resistance, wear

resistance, compressive strength, close tolerances, and a higher strength-to-weight ratio [246]. Heat treatment was performed on all workpieces at an outdoor heat treatment facility (maker: Metals Heat Treatment, India) to obtain an industrial application-based hardness of 58 ± 2 HRC. Initially, each workpiece was steadily preheated up to 650°C and held until uniform heating of each workpiece was achieved, then heated for 90 minutes in the vacuum furnace (maker: SECO-WARWICK, India), and finally cooled in oil quench. This furnace was powered by 230 V at 50 Hz, and the quenching pressure was kept between 5-8 bar. Technical specifications for the vacuum furnace include a working zone size of 610 × 750 × 1000 mm and a maximum temperature of 1,250°C. Lastly, to relieve residual stresses caused by quenching, workpieces were primary tempered at 400°C for 120 minutes, and secondary tempered at 450°C for 120 minutes. The elemental composition of the workpiece material was assessed by X-ray fluorescence (XRF) spectroscopy (maker: Bruker, model: S4 Pioneer), as shown in Table 3.1. As received workpiece material, it is typically in an annealed state, with fine carbides dispersed in a ferrite matrix. During heat treatment, samples were heated above austenitizing temperature and quenched, causing carbides in the matrix to dissolve and martensite structure to form.

Table 3.1 Chemical composition of the AISI D2 tool steel (wt.%).

Elements	C	Cr	Si	Mn	Mo	V	Fe
Weight %	1.55	11.80	0.30	0.40	0.90	0.80	Balance

Also, each sample underwent a primary and secondary tempering operation to improve its toughness. This procedure induces the formation of tempered martensite and a few carbides in the matrix structure. Figure 3.2 (a-c) depicts the AISI D2 tool steel workpiece sample, microstructure phases, and XRD pattern, respectively. Figure 3.2 (c) presents the X-ray

diffraction patterns of as received and hardened AISI D2 tool steel. Examination of the diffraction pattern for as received AISI D2 tool steel revealed peaks corresponding to the ferrite phase and iron-chromium carbide (M_7C_3). Following the heat treatment process, the XRD pattern of hardened AISI D2 tool steel exhibits three primary phases within the matrix: austenite, martensite, and M_7C_3 carbide. The presence of austenite is primarily attributed to the stability of the γ phase, which is influenced by the increased weight percentages of C and Cr in the solid solution.

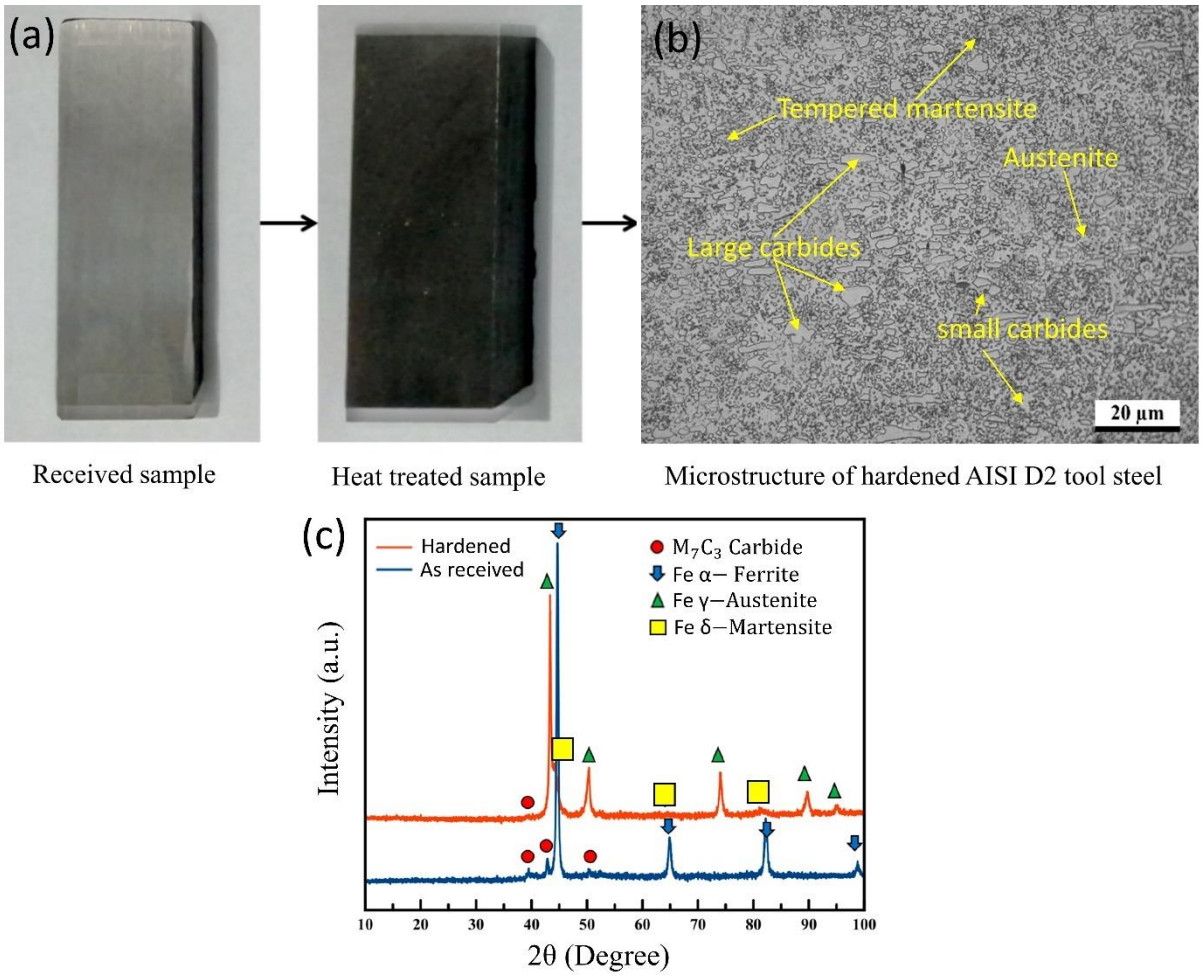

Figure 3.2 AISI D2 tool steel (a) Workpiece sample, (b) Microstructure, and (c) XRD pattern

3.2 Grinding machine and grinding wheel

The grinding experiments were conducted using a precision surface grinding machine (maker: Hindustan Machine Tool Ltd., H-455) with attached coolant and lubrication system with following specification the cone-shaped nozzle with a 10 mm output diameter was used to provide twenty percent water-based cutting fluid to the grinding zone at a flow rate of 1.5 litres per minute. The white alumina vitrified bond grinding wheel (maker: Carborundum Universal Ltd.) of dimension 250 mm × 20 mm × 76.2 mm with a wheel signature of AA60K5V6 was used in this work. The detail specification of the alumina wheel is as follows: grit size: 60 mesh; structure: dense; wheel hardness: medium; highest linear velocity: 60 m/s; binding agent: vitrified. All the grinding experiments have been performed in down grinding mode keeping equal spark-out passes. Further, carbon tape was used to collect the grinding chips. To maintain the uniformity in the wheel topography, grinding wheel was dressed with a single-grit non-rotating diamond dresser of size one carat (1 carat = 0.2 g). Dressing of the grinding wheel was performed with a dressing lead of 0.15 mm/rev, dressing speed of 39.42 m/s, and dressing depth of 40 μm with incremental dressing depth of 10 μm. A continuous flow of soluble oil has been supplied during wheel dressing to restrict any thermal damage to the diamond dresser, as diamond is extremely sensitive to high heat.

3.3 Single grit grinding experimental setup

An experimental study of single alumina abrasive grit grinding was designed and performed to validate the finite element analysis (FEA) model and the reliability of the simulated outcomes. Grinding forces during the single alumina abrasive grit in conventional dry grinding (CDG), and ultrasonic vibration assisted dry grinding (UVADG) modes were measured and compared with simulated results. Figure 3.3 (a, b) presents the CAD model of single grit grinding process and actual experimental setup for CDG and

UVADG modes, respectively. The single grit grinding experiments were performed using a surface grinding machine with single alumina abrasive grit (maker: Hitech Ceramics) with grit size #60. An alumina abrasive grit was glued over the grit holder block with Loctite super glue attached with carbon steel wheel. Figure 3.3 (b) clearly shows the alumina grit holder block, and the balance mass were symmetrically positioned in the steel wheel to improve the stability to outward force and get better location accuracy.

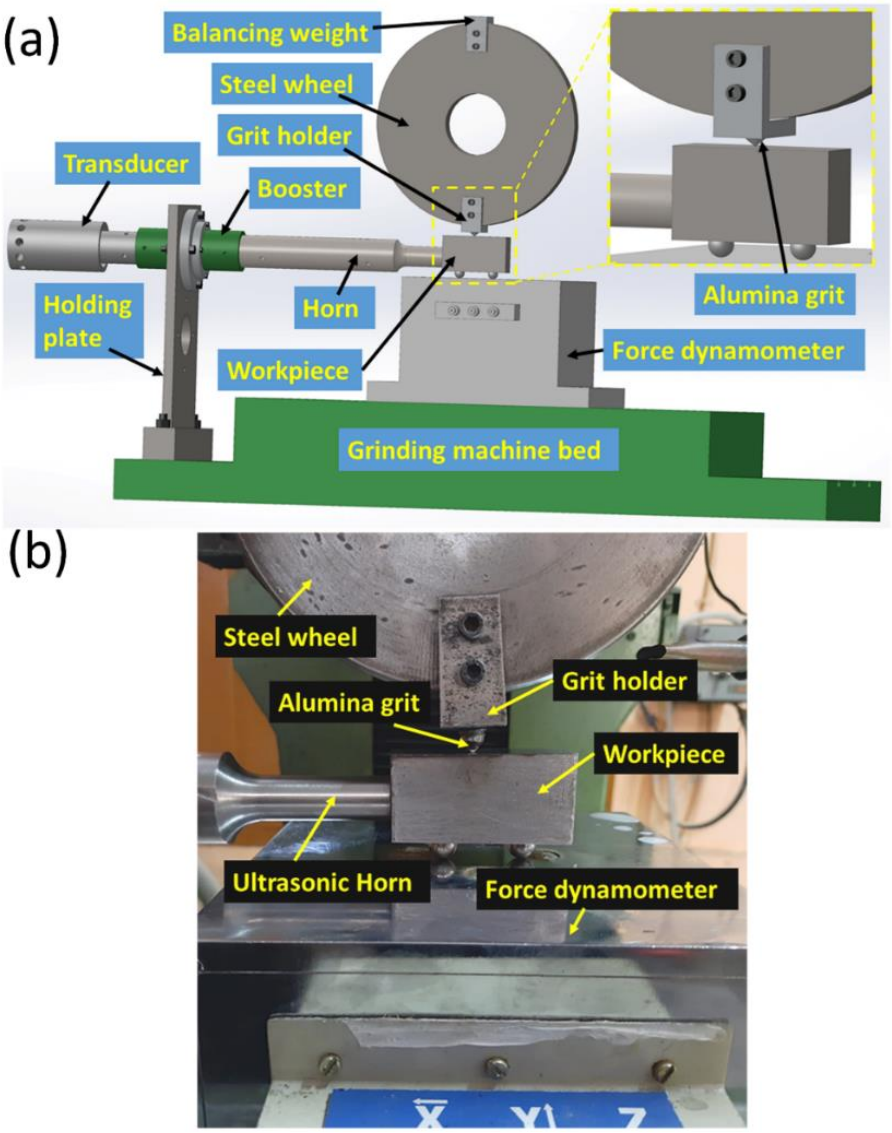

Figure 3.3 (a) 3D CAD model of UVADG setup (b) Actual UVADG experimental setup

Further, the balancing of the wheel is verified after inserting the attachment and counter attachment for fixing the single grit by using a dynamic balancing machine. This machine measures the imbalance of the wheel and automatically adjusts the position of the balance weights to minimize the imbalance. The use of a dynamic balancing machine ensures that the wheel rotates smoothly and without vibration, which is essential for achieving high-precision grinding results. An AISI D2 tool steel workpiece of dimension $60^{L}\times40^{T}\times20^{W}$ mm were used in this study. For establishing consistency in all experiments, precision grinding was performed before each experiment. A three-dimensional grinding force dynamometer (maker: IEICOS, Model-610C) was used to measure the tangential and normal grinding force.

As illustrated in Figure 3.3 (a), the schematic of the experimental UVADG setup consisting of the piezoelectric transducer, booster, titanium horn, and workpiece. The ultrasonic vibration amplitude used in the experimental work was in the order of a micron. The single grit UVADG system was calibrated before the tests using the standard technique for measuring grinding force.

3.4 Ultrasonic vibration assisted grinding experimental setup

As demonstrated in Figure 3.4 (a), the precision surface grinding machine combined with the coolant and lubrication system was used to conduct grinding experiments. Each experiment group was conducted in plunge grinding mode settings for 12 passes with repetition three times to minimise the random test errors, and the average value was computed. After each group grinding operation, the grinding wheel was dressed with a one carat single point diamond dresser to ensure all the experiments were consistent. Based on preliminary tests, four downfeed (10, 20, 30, and 40 µm), wheel velocity (39.42 m/s), and table feedrate (9 mm/min) were chosen for grinding AISI D2 tool steel workpiece (dimension: $80^{L}\times10^{T}\times15^{W}$ mm). The tangential and normal grinding forces were

measured using a three-dimensional grinding force dynamometer. The workpiece was fastened into the workpiece holding fixture before being placed on the dynamometer. The indigenously developed UVAG setup was calibrated before performing the tests using a standard method for grinding force computation based on standard procedure. The UVAG system components are shown in detail in Figure 3.4 (a): actual experimental setup for UVAG and Figure 3.4 (b): schematic of the 3D UVAG setup. The supplied electrical energy (50 Hz) to the ultrasonic generator (maker: Ultra Autosonic India) was first transformed into mechanical vibration of 21 kHz via a piezoelectric transducer. The ultrasonic transducer then delivers ultrasonic tangential vibration at the matching frequency. After that, the tangential vibration was subsequently amplified with a booster and a titanium horn. The workpiece holding fixture was joined with the titanium horn and kept on the force dynamometer by two supporting frictionless balls to diminish the vibration loss. The tangential vibration amplitudes on the workpiece were controlled, varied, and measured with the help of laser displacement sensor and controller (maker: Keyence, Model: LK-G32). This experiment used the same setup for UVADG, CDG, and CWG modes to carry out the tests. In the CWG mode, the cone-shaped nozzle with a 10 mm output diameter was used to provide twenty percent water-based cutting fluid to the grinding zone at a flow rate of 1.5 litres per minute. However, during conventional grinding, ultrasonic power was shut down.

As demonstrated in Figure 3.4 (c), the trajectory of conventional grinding is linear, while ultrasonic grinding pursues a sine waveform trajectory due to the ultrasonic vibration on the workpiece. The direction of ultrasonic vibration is tangential to the worktable feed rate. The ultrasonic vibration assisted grinding process has a periodic reciprocating motion, which results in the discontinuous cutting action of abrasive grits.

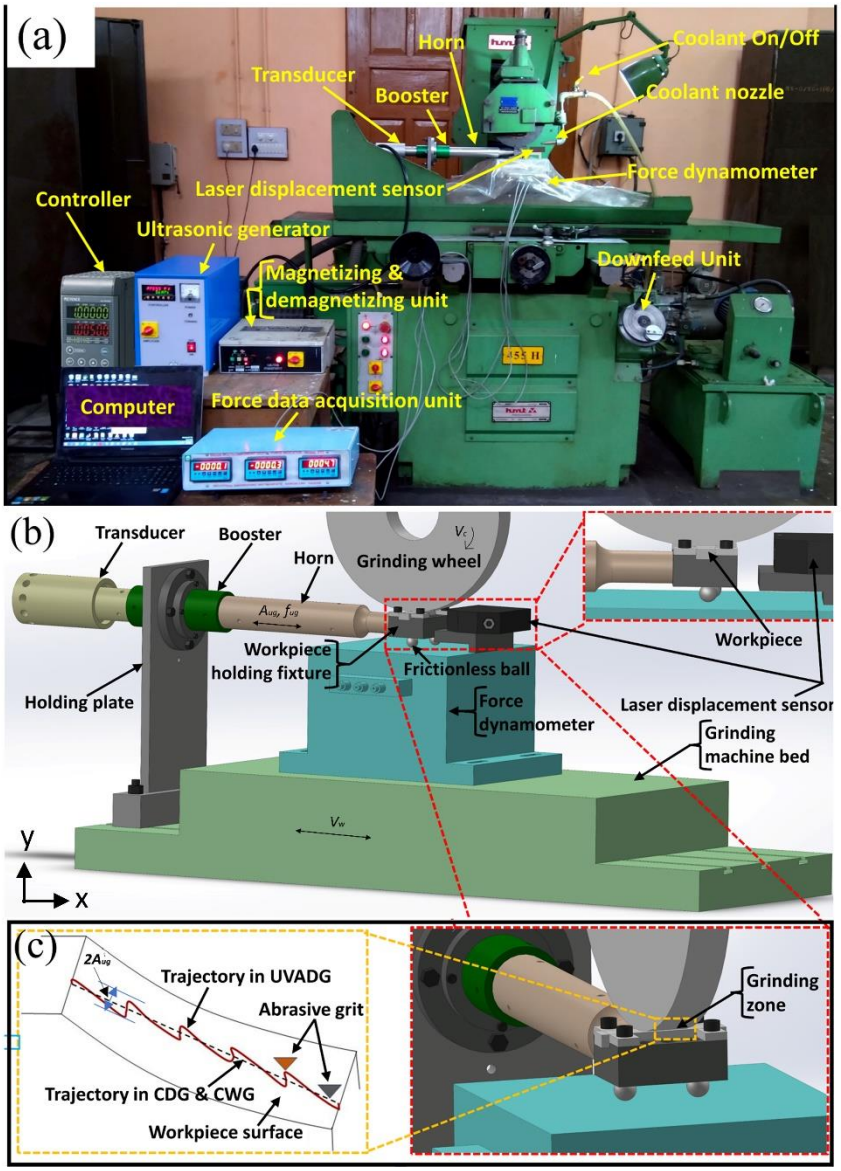

Figure 3.4 The experimental setup for surface grinding (a) Actual experimental setup for UVAG (b) Schematic of 3D UVAG setup (c) Grinding zone and trajectory of abrasive grit

3.5 Ultrasonic vibration assisted minimum quantity lubrication (UVAMQL) grinding setup

Ultrasonic vibration assisted minimum quantity lubrication grinding (UVAMQL) was performed in an indigenously developed setup illustrated in Figure 3.5 (a-b). The ultrasonic generator (maker: Ultra Autosonic India) was used to transform the supplied electrical energy into mechanical vibration at an ultrasonic frequency of 21 kHz with a piezoelectric

transducer. The ultrasonic transducer then delivers ultrasonic tangential vibration at the matching frequency. A booster and a titanium sonotrode were later employed to intensify the vibration. In order to minimise vibration losses, two supporting frictionless balls were used and maintained the workpiece retaining fixture on the force dynamometer while it was attached to the titanium sonotrode. The vibration amplitudes on the workpiece were regulated, changed, and monitored using a laser displacement sensor and controller (maker: Keyence, Model: LK-G32). A custom minimum quantity lubrication grinding (MQL) setup was fabricated using a movable attachment on the grinding wheel cover of the surface grinding machine, as shown in Figure 3.5 (a-b). An economical MQL system is built by combining an air-atomizing spray nozzle with an attached bevel protractor, a pressure gauge, a pressure regulator, a flow control valve, and an air compressor (maker: Powerhouse, model-PH1530). An external mixing type air atomizing spray nozzle (maker: Spraytech Systems Pvt. Ltd.) with an orifice size of 1 mm was used to produce a fine mist spray in the grinding zone. A gravitational head principle is used to feed cutting fluid to the spray nozzle, along with the help of high-pressure compressed air. As MQL nozzle position, i.e., stand-off distance (Z), nozzle angle (α), and MQL flow parameters, i.e., flow rate (Q), air pressure (P), considerably affect the cooling and lubrication performance of the MQL system. Therefore, before beginning the actual experiments, several preliminary tests were conducted to determine the MQL system's optimum parameters for our setup. Four types of cutting fluids, i.e., vegetable oil, oil-water emulsion and nanofluids with two weight percentages, were used in the experiments as MQL cutting fluids. The MQL parameters for vegetable oil are Q = 200 ml/h, P = 4 bar, $\alpha = 12^{\circ}$ and Z = 50 mm. The MQL parameters for oil-water emulsion and nanofluids are Q = 150 ml/h, P = 4 bar, $\alpha = 12^{\circ}$ and Z = 40 mm. The experimentation was performed employing a precision surface grinding. A white alumina grinding wheel was used in the present experiment.

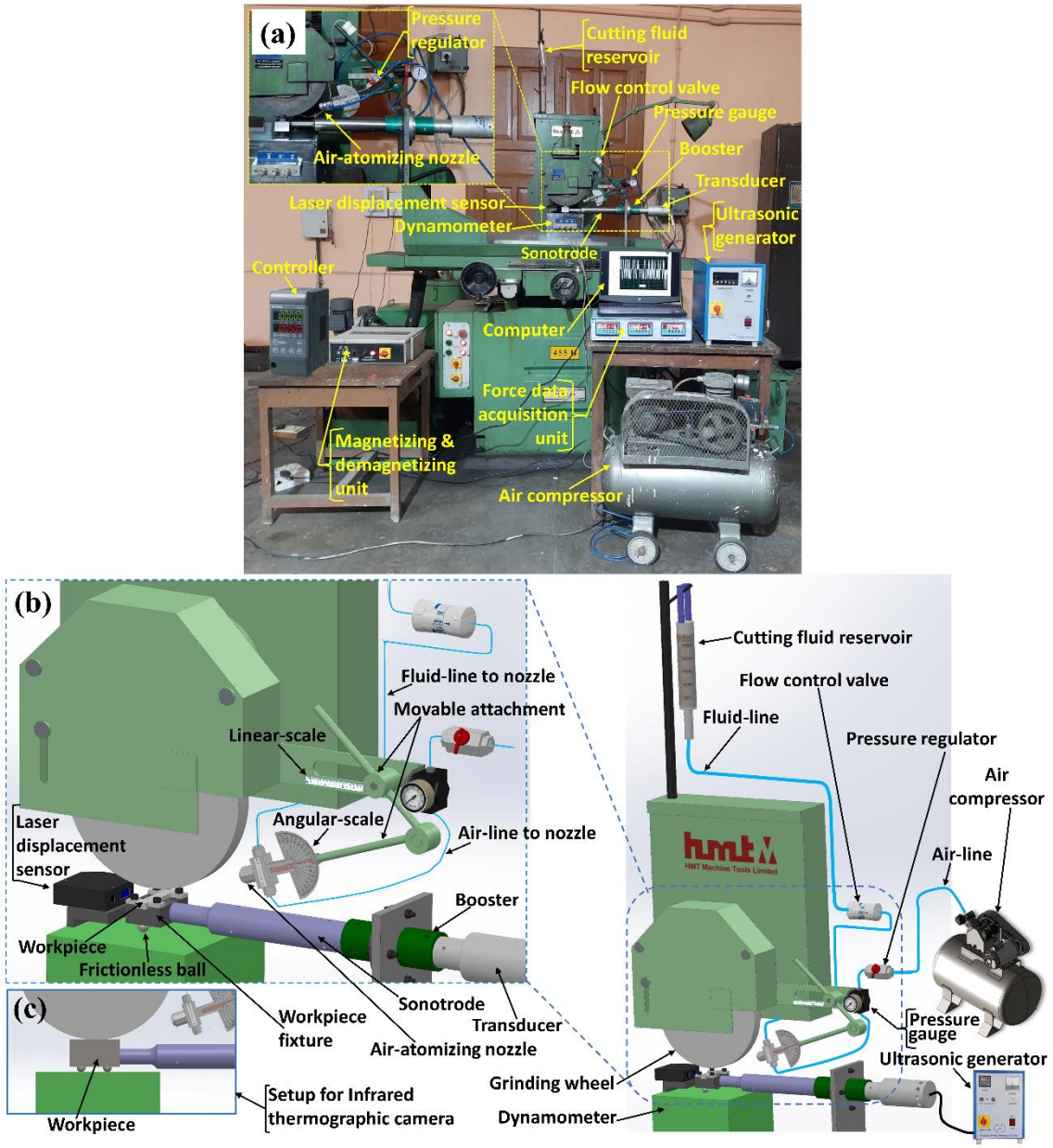

Figure 3.5 (a) Actual experimental UVAMQL grinding setup, (b) Schematic of 3D UVAMQL grinding setup, (c) Setup for high-speed infrared thermographic camera to measure the grinding temperature

For the dry, MQL, and UVAMQL grinding tests, the same setup was used, and during the dry and MQL grinding tests, the ultrasonic power was turned off. To reduce random test errors, each grinding experiment was run in plunge grinding mode for five passes with three repetitions, and the average value was calculated. To confirm that all the tests were uniform, the grinding wheel was dressed with a one-carat single-point diamond dresser after each

group grinding operation. Based on the preliminary experiments for grinding an AISI D2 tool steel workpiece under dry, MQL, and UVAMQL grinding environments, the optimal grinding parameters were selected, such as a worktable feed rate of 9 m/min, wheel velocity of 39.42 m/s, downfeed of 30 µm. The 3D grinding force dynamometer was used to compute the tangential and normal grinding forces.

3.6 Calibration of experimental grinding setup

The standard procedure was used in this work as follows. We have calibrated the ultrasonic vibration-assisted grinding setup for grinding force measurement before conducting the actual experiments. Figure 3.6 (a) shows that ultrasonic vibration is off without putting a 5kg load on the workpiece, and the force data acquisition unit displays zero grinding force reading. Besides, Figure 3.6 (b) shows that ultrasonic vibration is off with just slowly putting a 5kg load over the workpiece, and the force data acquisition unit displays a 5kgf (~50N) normal grinding force reading, which indicates that the proper design and develop an ultrasonic vibration assisted grinding setup for assessment of grindability and surface integrity of AISI D2 tool steel.

The minimization of friction is a crucial consideration in our experimental setup. To address this, both the resting platform and the work-holding fixture, which are in contact with highly smooth-finished steel balls, are specially mirror-finished surfaces. This ensures that friction between the steel balls and these two surfaces is almost negligible due to the point-contact support at the interface. After complete assembly, the experimental setup undergoes thorough calibration through a series of trial runs. These trials serve to refine the vibration parameters and ensure optimal performance. Throughout the experimental grinding setup, two highly finished steel balls are employed to provide point contact support.

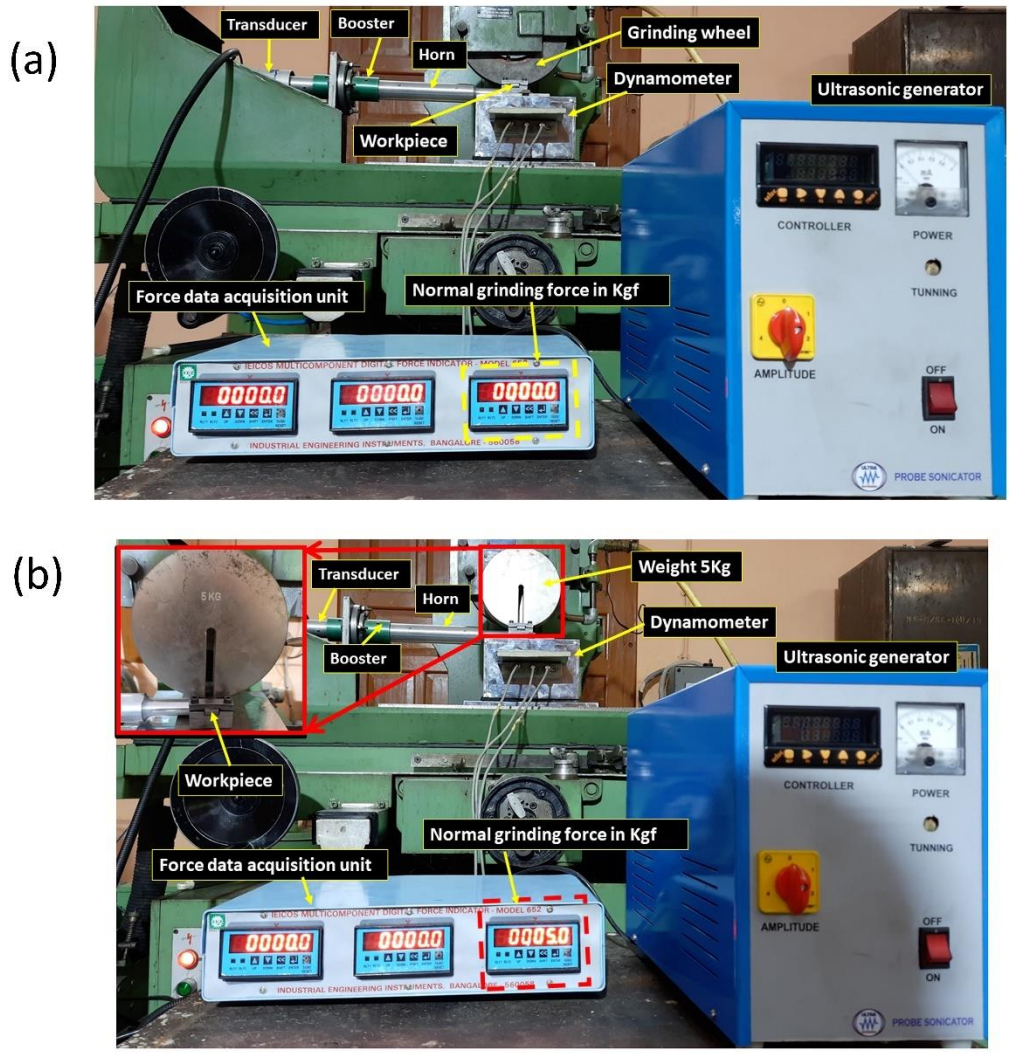

Figure 3.6 (a) Without putting 5kg load on the workpiece, (b) With just slowly putting 5kg load on the workpiece

3.7 Grindability and surface integrity indices

3.7.1 Measurement of grinding force and specific grinding energy

To study the grinding behaviour of any engineering material, grinding force measurement is crucial. The magnitude of the grinding forces provides direct data on the performance of the grinding process, including analysis of the wheel loading behaviour and forecasting of the temperature, specific grinding energy, coefficient of friction, and surface roughness. Using a three-dimensional grinding force dynamometer (maker: IEICOS, Model-610C),

the tangential (F_t) and normal (F_n) grinding forces in the present work have been measured. A multi-channel charge amplifier and data collection software called MDFIS (Model 652) are connected to the dynamometer. The grinding forces can be measured by this dynamometer up to 1000 Newton with a response time of one millisecond. Accurately estimating the friction coefficient is next to impossible due to the dynamic and complex nature of the grinding process. In order to calculate the apparent coefficient of friction, the tangential force to normal force ratio was used. The fundamental quantity known as specific grinding energy, which is defined as the amount of energy used to remove a unit volume of material, is obtained from the power and grinding conditions. Instead, it is thought that low specific energy is more environmentally beneficial. Yet, compared to more general machining techniques like turning and milling, the specific energy used during grinding is over twofold greater. This is caused by the exceptionally high dislocation densities created by very small grinding chips in the shear zone, as well as by the energy used in unfavourable rubbing and ploughing operations. Specific grinding energy (e_c) is calculated by equation (3.1).

$$e_c = \frac{F_t \times V_c}{V_w \times a_p} \tag{3.1}$$

where, F_t -tangential force (N), V_c -wheel speed (m/s), a_p -downfeed (μm), , and V_w -worktable feed rate (mm/min).

3.7.2 Measurement of grinding temperature

The heat generated in the grinding process is caused by the rubbing, ploughing, and shearing action of the abrasive wheel on the work material. When the grinding temperature exceeds a certain limit, thermal damage to the ground surface occurs in the form of oxidation, burning, and microcrack development. As a result, achieving the lowest possible grinding temperature in the cutting zone is the ultimate goal during grinding. As a result,

regulating the grinding temperature is critical to preserving the surface integrity of samples. A high-speed infrared thermographic camera (maker: FLIR-E75) having a 320×240-pixel infrared resolution and response time of 9 millisecond with an emissivity of 0.95 was used to measure the maximum grinding temperature of a workpiece. The workpiece dimension for the temperature measurement setup was $70^{L}\times20^{T}\times50^{W}$ mm (refer to Figure 3.5 (c)), and a high-speed infrared thermographic camera was placed at the optimal distance of 550 mm from the front face of the workpiece for measurement of grinding temperature as shown in the Figure 3.7 (a-b).

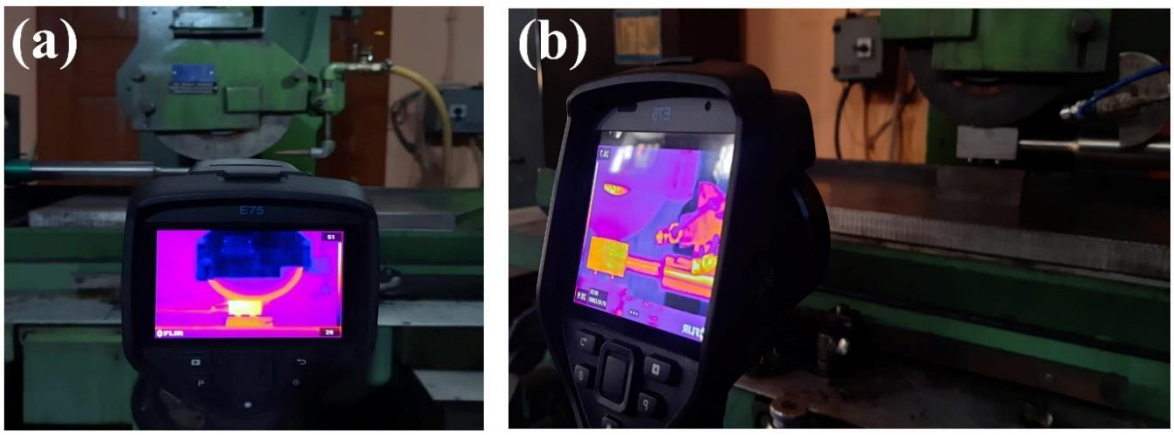

Figure 3.7 High-speed thermographic camera arrangement, (a) UVAG temperature measurement, (b) UVAMQL grinding temperature measurement

3.7.3 Measurement of surface roughness

Surface roughness is one of the essential criteria that must be thoroughly investigated in order to analyse the surface integrity of the ground surface. Surface roughness is considered in this work in accordance with the internationally known ISO 4287:1977 standard [15]. The ground workpiece was cleaned in an ultrasonic bath with ethanol for 10 min following the grinding operations. A 2D surface profilometer (maker: Mitutoyo, Model: SV-2100-S4) was utilized to measure the surface roughness (R_a, R_q and R_z) at three distinct places on the ground surface perpendicular to the grinding direction. An algorithm called a low-pass Gaussian filter was used to get the average line roughness out of the raw profile having

traverse length (4 mm) and cut-off length (0.8 mm). A cantilever type probe with a diamond stylus of radius 2 μm is used to obtain ground surface profiles. Even under extremely low loads, the hard diamond stylus may leave a micro-indent on the work surface while tracing the surface profile. According to ISO 3274: 1996, the static measurement force at the mean location of the stylus should be 0.75 mN. This force is normally determined by the instrument's manufacturer. If the force value is a problem, the stylus can be loaded onto an appropriate pan-balance [15].

3.7.4 Scanning electron microscope (SEM) and atomic force microscope (AFM) analysis

Surface integrity has a substantial impact on the service life of manufactured components, as poor surface integrity can lead to component failure during its service life. Consequently, the surface integrity of the ground samples has been investigated using various surface characterization techniques, such as SEM and AFM. Using an electron beam, SEM is able to image a ground surface. The electron beam interacts with the surface of the sample, and topographic images of the surface can be obtained using a suitable detector. In the present study, the morphology of the ground workpiece was analysed using the SEM (maker: Zeiss, model: EVO-18-Research). The measurements have been carried out with a 20 kV accelerating voltage. Furthermore, microchip morphology has been analysed with the help of SEM. The nanoscale 3D surface topography such as average surface roughness (S_a), root mean square surface roughness (S_q), average peak to valley height (S_t), and bearing area curve parameter values of the ground workpiece were obtained using an AFM (maker: NT-MDT, model: NTEGRA PRIMA). The same area of all ground samples was scanned for AFM imaging. For surface morphology and topography analysis, all ground workpieces were cut perpendicular to the ground surface using wire electrical discharge machining

(maker: Medha Ent, model: Expresscut-Ex4032C) in a square shape (dimension: 10 × 10 mm) to prevent thermal damage to the workpiece while the cutting process.

3.7.5 Metallographic and microhardness analysis

For metallographic and microhardness studies, all samples were cut perpendicular to the grinding direction using wire electrical discharge machining to a size of 10 × 10 mm. The standard metallographic procedure was used to produce specimens (ASTM E3-11). These specimens were successively hot moulded in a specimen mount press (maker: Chennai Metco Pvt. Ltd.) with the help of bakelite powder. Moulded samples were polished on SiC emery papers with successively finer meshes of 120, 320, 600, 800, 1000, and 1200, followed by cloth polishing with alumina slurry on an auto-disc polishing machine (maker: Chennai Metco Pvt. Ltd.). All samples were etched using a 5% nital solution for approximately 15 seconds. Under a metallurgical optical microscope (maker: Dewinter Technologies, Classical PL), the microstructure of the ground surface was examined after being promptly rinsed with running tap water and dried with a hand-held electric blower.

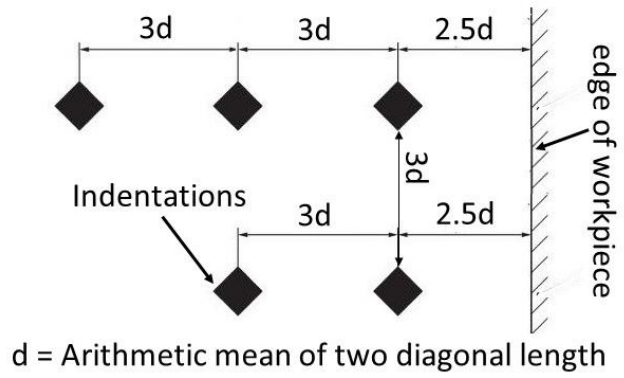

Figure 3.8 Minimum distance of two Vickers indentations for steel

The microhardness measurements were carried out along the subsurface and ground surface with an applied load of 100 g and a dwell time of 10 seconds using a Vickers microhardness

tester (maker: Micromech Technologies, SN-104). At three locations, the Vicker indentation began at a depth of 25 μm and extended to a maximum depth of 300 μm. For analysis, the average values of microhardness measurements were considered. In this study, an international normative (International Standard ISO 6507-1) is used for microhardness measurement, as shown in Figure 3.8. Generally, the distance between two indentations is equal to two times of previous location indentation size because of the plastic deformation of a localised region.

3.8 Physical characterization of different UVAMQL lubricants

3.8.1 Measurement of thermal conductivity, viscosity, wettability, and surface tension of lubricants

The effectiveness of any eco-friendly cutting fluid in UVAMQL grinding mainly depends on its cooling and lubricity behaviour. Therefore, the cooling and lubricating properties of the prepared soyabean oil-deionized water (SO+DW) emulsion and nanofluid need to be quantified before their application to a grinding process. Such quantification will be helpful in recommending their possible favourable mechanisms while grinding. Consequently, SO+DW emulsion and Al_2O_3 NFs have been characterised through the measurement of thermal conductivity, viscosity, and wettability. Thermal conductivity, a measure of a solid or liquid ability to conduct heat, is an important property for thermal analysis. A thermal constant analyzer (maker: Hot Disk, TPS-500) measured the thermal conductivity of sustainable cutting fluids by the transient plane source principle (refer to Figure 3.9 (a)). The sensors used contained nickel foil embedded between two thick layers of Kapton polyimide film. The nickel foil wound in a double spiral pattern has a radius of 3.189 mm. While passing the heating power, spherical waves are generated through the probe end that travels through the sample. The hot disk measures the thermal conductivity and thermal resistivity, for a constant heating rate, from the rate of temperature increase of the probe.

The thermal conductivity of fluids in the range of 0.2–2 W/mK with an accuracy of ±1.5% can be measured.

Viscosity is one of the most important physical properties of lubricants. It describes the internal resistance of a fluid to deformation. It has a direct influence on the lubricity behaviour of the lubrication film that forms between the grinding wheel and work surface. The viscosity of the cutting fluids was measured by a viscometer (maker: Brookfield Digital Rheometer, DV1-Cone & Plate Version) with a temperature bath to set the room temperature (25 °C). The operating principle of the viscometer is to drive a spindle connected to a plate immersed in the test fluid via a calibrated spring. The spring deflection measures the viscous drag force of the fluid against the plate and spindle. This system provides continuous sensing and display of the measurement during the entire test. Generally, low-viscosity fluids require spindles with larger surface areas and high rotational speeds. The spindle used was CP42, which is used for samples with a viscosity starting at 0.3 cP. The minimum amount of fluid required for viscosity measurements is 1.0 mL.

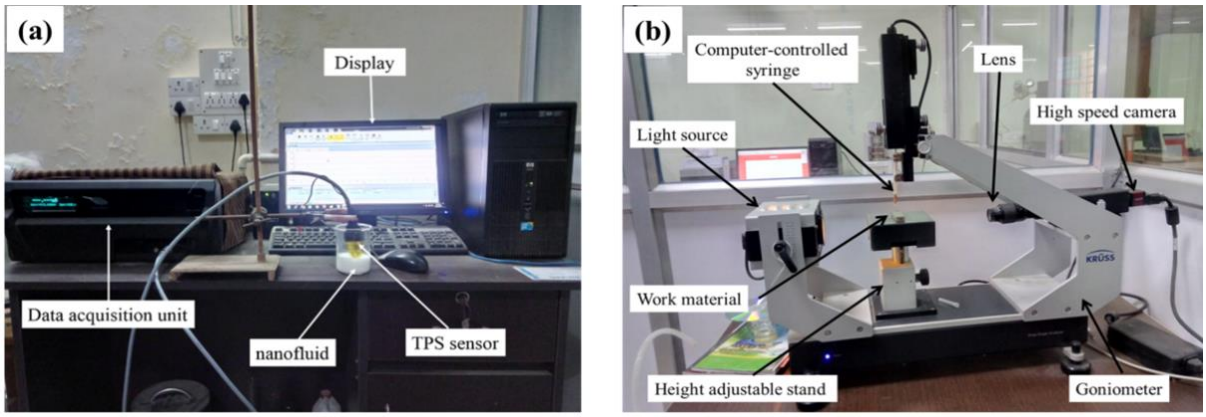

Figure 3.9 (a) Thermal constant analyzer, (b) Drop shape analyzer

Wettability studies usually involve the measurement of fluid contact angles with respect to a solid interface. Contact angles play a major role in quantifying the flowability and the

lubricating behaviour of a colloidal suspension on the work surface. The contact angle is defined as the angle formed by the intersection of the liquid-solid interface and the liquid-vapour interface. The contact angles are geometrically acquired by applying a tangent line from the contact point along the liquid-vapour interface in the droplet profile. Contact angles using the sessile drop technique of prepared nanosuspension fluids on the AISI D2 tool steel surface has been measured with the help of a drop shape analyzer (maker: KRUSS Scientific, DSA25S) with a dropping rate of 1 μL/s and precision of 0.1°. The contact angles have been measured using the principle given by Thomas Young [247]. The photographic view of the goniometer arrangement for cutting fluid is shown in Figure 3.9 (b).

Surface tension is a phenomenon that describes the difference in interfacial energy between molecules at a fluid interface and their bulk counterparts at the molecular level [248]. It has a very important role in deciding the boiling, spreading, and spray characteristics of a fluid. The surface tension of the various cutting fluids was evaluated using a drop shape analyzer with the pendant drop method. This approach analyses the droplet shape suspended from a syringe based on the equilibrium of intermolecular forces using the Young-Laplace model, which provides the fluid surface tension. The surface tension can be calculated to the drop shape by following empirical Eq^{n} (3.2) and (3.3) given by Berry et al. [248].

$$\sigma' = \frac{g D_e^2 \Delta\rho}{H} \tag{3.2}$$

$$S = \frac{D_s}{D_e} \tag{3.3}$$

where σ' is the interfacial tension, $\Delta\rho$ is the density difference between the fluid phases, D_e is the equatorial diameter of the drop (Figure 3.10), H is a correction factor which is related to the shape factor of the pendant drop S, the drop diameter measured horizontally i.e., D_s.

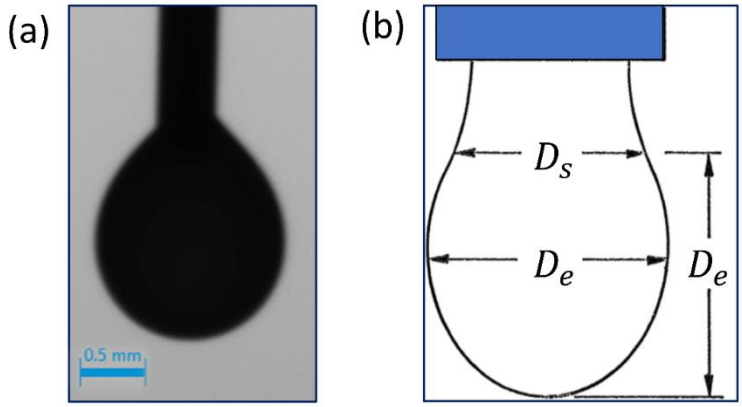

Figure 3.10 Pedant drop geometry (a) Actual, (b) Schematics

For the purpose of producing the 1/H vs. S curve, Drelich et al. [249] have established six empirical equations (Eq^{n} 3.4 to 3.9). To estimate the correlation parameter 1/H, use the shape factor listed below. Using the pendant drop technique, the equations help to determine the surface tension. The equations hold true for S values in the range of 0.3 to 1.

for S = 0 0.300 to S = 0 0.400

$$\frac{1}{H} = \frac{0.34074}{S^{2.52303}} + 123.9495 \times S^5 - 72.82991 \times S^4 + 0.01320 \times S^3 - 3.38210 \times S^2 + 5.52969 \times S - 1.07260 \quad (3.4)$$

for S > 0.400 to S = 0.460

$$\frac{1}{H} = \frac{0.3272}{S^{2.56651}} - 0.97553 \times S^2 + 0.84059 \times S - 0.18069 \quad (3.5)$$

for S > 0.460 to S = 0.590

$$\frac{1}{H} = \frac{0.31968}{S^{2.59725}} - 0.46898 \times S^2 + 0.50059 \times S - 0.13261 \quad (3.6)$$

for S > 0.590 to S = 0.680

$$\frac{1}{H} = \frac{0.31522}{S^{2.62435}} - 0.11714 \times S^2 + 0.15756 \times S - 0.05285 \quad (3.7)$$

for S > 0.6800 to S = 0.900

$$\frac{1}{H} = \frac{0.31345}{S^{2.64267}} - 0.09155 \times S^2 + 0.14701 \times S - 0.05877 \quad (3.8)$$

for S > 0.900 to S = 1.000

$$\frac{1}{H} = \frac{0.30715}{S^{2.84636}} - 0.69116 \times S^3 + 1.08315 \times S^2 - 0.18341 \times S - 0.20970 \quad (3.9)$$